

Power corrections to the $\pi^0\gamma$ transition form factor and pion distribution amplitudes

S. S. Agaev*

*High Energy Physics Lab., Baku State University,
Z. Khalilov st. 23, 370148 Baku, Azerbaijan*

(Dated: November 25, 2018)

Abstract

Employing the standard hard-scattering approach and the running coupling method we calculate a class of power-suppressed corrections $\sim 1/Q^{2n}$, $n = 1, 2, 3 \dots$ to the electromagnetic $\pi^0\gamma$ transition form factor (FF) $Q^2 F_{\pi\gamma}(Q^2)$ arising from the end-point $x \rightarrow 0, 1$ integration regions. In the investigation we use a hard-scattering amplitude of the subprocess $\gamma + \gamma^* \rightarrow q + \bar{q}$, symmetrized under the exchange $\mu_R^2 \leftrightarrow \bar{\mu}_R^2$ important for exclusive processes containing two external photons. In the computations the pion model distribution amplitudes (DA's) with one and two nonasymptotic terms are employed. The obtained predictions are compared with the CLEO data and constraints on the DA parameters $b_2(\mu_0^2)$ and $b_4(\mu_0^2)$ at the normalization point $\mu_0^2 = 1 \text{ GeV}^2$ are extracted. Further restrictions on the pion DA's are deduced from the experimental data on the electromagnetic FF $F_\pi(Q^2)$.

PACS numbers: 12.38.Bx, 13.40.Gp, 14.40.Aq

*Electronic address: agaev'shahin@yahoo.com

I. INTRODUCTION

The π^0 meson electromagnetic transition form factor (FF) $F_{\pi\gamma}(Q^2)$ is among the simplest exclusive processes for investigation of which at large momentum transfer the perturbative QCD (PQCD) methods [1, 2, 3] can be applied. Because of the recent CLEO data [4], where the form factor $F_{\pi\gamma}(Q^2)$ was measured with high precision, the interest in this process has been renewed. Thus during the last few years for computation of $F_{\pi\gamma}(Q^2)$ the various theoretical methods and schemes were proposed [5, 6, 7, 8, 9]. The aim here is twofold: to elaborate methods for the calculation of $F_{\pi\gamma}(Q^2)$ within PQCD and, at the same time, to extract from experimental data information on the pion distribution amplitude (DA). The latter, being independent of a specific exclusive process and universal quantity, is an important input ingredient in studying various processes that involve the pion.

It is known that in experiments the $\pi^0\gamma$ transition was explored at momentum transfers of $Q^2 \sim 1 - 10 \text{ GeV}^2$, which are far from the asymptotic limit $Q^2 \rightarrow \infty$, where the PQCD factorization formula with the pion leading-twist asymptotic DA leads to reliable predictions. In the present experimentally accessible energy regimes, power-suppressed corrections $\sim 1/Q^{2n}$, $n = 1, 2, \dots$ play an important role in explaining the experimental data [5, 9]. There are numerous sources of power corrections to $F_{\pi\gamma}(Q^2)$. For example, the pion higher-twist (HT) DA's and higher Fock states generate such corrections. Power corrections can also originate from the end-point regions $x \rightarrow 0, 1$ as a result of the integration of the PQCD factorization expression with the QCD running coupling $\alpha_s(Q^2x)$ [$\alpha_s(Q^2\bar{x})$, $\bar{x} = 1-x$] over the pion's quark longitudinal momentum fraction x . In fact, in order to reduce the higher-order corrections to a physical quantity and improve the convergence of the corresponding perturbation series, the renormalization scale μ_R^2 ($\bar{\mu}_R^2$), i.e., the argument of the QCD coupling, in a Feynman diagram should be set equal to the virtual parton's squared four-momentum [10]. In the exclusive processes the scale μ_R^2 ($\bar{\mu}_R^2$) chosen this way inevitably depends on the longitudinal momentum fractions carried by the hadron constituents. For the photon-meson transition we have $\mu_R^2 = Q^2x$ and $\bar{\mu}_R^2 = Q^2\bar{x}$, because at two leading order diagrams of the partonic subprocess $\gamma + \gamma^* \rightarrow q + \bar{q}$, absolute values of the virtual quark and antiquark squared four-momenta are determined by these expressions. But then the PQCD factorization formula diverges, since $\alpha_s(Q^2x)$ [$\alpha_s(Q^2\bar{x})$] suffers from end-point $x \rightarrow 0$ [$x \rightarrow 1$] singularity. The running coupling (RC) method solves this problem by using a Borel transformation and applying the principal value prescription. As a result, one obtains the Borel resummed expression for the $\pi^0\gamma$ transition FF, which contains power-suppressed corrections. The RC method in conjunction with the infrared (IR) renormalon calculus was used for computation of such power corrections to the $\pi^0\gamma$ and $\eta\gamma, \eta'\gamma$ transition FF's [5, 9], to the electromagnetic FF's of the light mesons $F_M(Q^2)$ ($M = \pi, K, \rho_L$) [11, 12, 13, 14], as well as to the gluon-gluon- η' meson vertex function [15].

In the present work we compute power corrections to the $\pi^0\gamma$ transition FF employing the version of the hard-scattering amplitude symmetrized under replacement $\mu_R^2 \leftrightarrow \bar{\mu}_R^2$. The symmetrization procedure is important for exclusive processes with two external photons (gluons) in the hard-scattering Feynman diagrams, because it allows one to treat within the RC method both virtual and real photons (gluons) on the same footing. The latter is required in order to consider the $\pi^0\gamma^*$ and $\pi^0\gamma$ transitions in a unifying way, i.e., to get in the limits $\omega \rightarrow 0; 1$ (ω is the asymmetry parameter) from the $\pi^0\gamma^*$ transition FF $F_{\pi\gamma^*}(Q^2, \omega)$ the FF $F_{\pi\gamma}(Q^2)$ of the $\pi^0\gamma$ transition. The advocated method was used in our previous work [15] to investigate the virtual and on-shell gluon- η' meson transitions. In what follows we

refer to this approach as the symmetrized RC (SRC) method.

This paper is organized as follows: in Sec. II we introduce the symmetrization procedure of the hard-scattering amplitude for the $\pi^0\gamma$ transition. Here we present our results for the Borel resummed $[Q^2 F_{\pi\gamma}(Q^2)]^{res}$ FF obtained within the SRC method. Section III is devoted to detailed analysis of the $Q^2 \rightarrow \infty$ limit of $[Q^2 F_{\pi\gamma}(Q^2)]^{res}$. In Sec. IV we perform numerical computations and from comparison of our predictions with the CLEO data extract constraints on the parameters $b_2^0(1 \text{ GeV}^2)$ and $b_2^0(1 \text{ GeV}^2)$, $b_4^0(1 \text{ GeV}^2)$ in the pion DA's with one and two nonasymptotic terms, respectively. Further restrictions on the DA's arising from analysis of the pion electromagnetic FF are described in Sec. V. In Sec. VI we make our concluding remarks.

II. THE PHOTON-MESON TRANSITION FORM FACTOR

A. The symmetrized version of the hard-scattering amplitude

The real photon-pseudoscalar M meson electromagnetic transition FF $F_{M\gamma}(Q^2)$ can be defined in terms of the amplitude $\Gamma^{\mu\nu}$,

$$\Gamma^{\mu\nu} = ie^2 F_{M\gamma}(Q^2) \epsilon^{\mu\nu\alpha\beta} P_\alpha q_{1\beta}, \quad (2.1)$$

for the process

$$\gamma^*(q_1) + \gamma(q_2) \rightarrow M(P), \quad (2.2)$$

where $Q^2 = -q_1^2$ is the momentum transfer.

At the large momentum transfer the FF $F_{M\gamma}(Q^2)$ is given by the factorization formula of the standard hard-scattering approach (HSA) [1],

$$F_{M\gamma}(Q^2) = [T_H^1(x, Q^2, \mu_F^2) + T_H^2(x, Q^2, \mu_F^2)] \otimes \phi_M(x, \mu_F^2). \quad (2.3)$$

Here the function $T_H(x, Q^2, \mu_F^2)$,

$$T_H(x, Q^2, \mu_F^2) = T_H^1(x, Q^2, \mu_F^2) + T_H^2(x, Q^2, \mu_F^2), \quad (2.4)$$

is the hard-scattering amplitude of the subprocess $\gamma + \gamma^* \rightarrow q + \bar{q}$, $\phi_M(x, \mu_F^2)$ is the meson DA, μ_F^2 is the factorization scale, and $\bar{x} \equiv 1 - x$, x being the longitudinal momentum fraction carrying by the meson's quark. In Eq. (2.3) the shorthand notation

$$T_H(x, Q^2, \mu_F^2) \otimes \phi_M(x, \mu_F^2) = \int_0^1 T_H(x, Q^2, \mu_F^2) \phi_M(x, \mu_F^2) dx \quad (2.5)$$

is used.

It is evident that a physical quantity, represented by the factorization formula, Eq. (2.3) being a sample one, does not depend on renormalization and factorization schemes and scales employed for its calculation. But at any finite order of the QCD perturbation theory, due to truncation of the corresponding perturbation series, the hard-scattering amplitude (2.4) depends on both the factorization μ_F^2 and renormalization μ_R^2 scales. Since higher-order corrections in PQCD computations, as a rule, are large for both inclusive and exclusive processes, in order to get reliable theoretical predictions within the PQCD by means of the truncated perturbation series, an optimal choice for these scales, i.e., a choice that

minimizes higher-order corrections, is required. The factorization scale μ_F^2 in exclusive processes is traditionally set equal to the momentum transfer Q^2 , because higher-order corrections contain terms $\sim \ln(\mu_F^2/Q^2)$ and such choice eliminates them in hard-scattering amplitudes. As a result, in the factorization formula only a hadron DA explicitly depends on the scale $\mu_F^2 = Q^2$.

The situation with the renormalization scale μ_R^2 is more subtle. Really, this scale appears, in general, not only in higher-order corrections to the hard-scattering amplitude, but also determines the scale of the QCD coupling $\alpha_s(\mu_R^2)$. In order to reduce higher-order corrections to a physical quantity, in exclusive processes the scale μ_R^2 should be taken equal to the square of the momentum transfer carried by a virtual parton in each leading order Feynman diagram of the underlying hard-scattering subprocess [10]. For the real photon-meson transition these scales are determined by the leading order diagrams of the subprocess $\gamma + \gamma^* \rightarrow q + \bar{q}$ and are given by the expressions

$$\mu_R^2 = Q^2 x, \quad \bar{\mu}_R^2 = Q^2 \bar{x}. \quad (2.6)$$

After these remarks let us turn to our formulas (2.3) and (2.4). In accordance with the "tradition," in this work we set $\mu_F^2 = Q^2$ and in what follows omit the dependence of the hard-scattering amplitude on the scale μ_F^2 . Then, for the hard-scattering amplitude at the next-to-leading order (NLO) we get [16]

$$T_H^1(x, Q^2, \mu_R^2) = \frac{N}{Q^2} \frac{1}{x} \left[1 + C_F \frac{\alpha_s(\mu_R^2)}{4\pi} t(x) \right], \quad (2.7)$$

where the function $t(x)$ is given by the expression

$$t(x) = \ln^2 x - \frac{x \ln x}{\bar{x}} - 9. \quad (2.8)$$

Here N is the constant, which depends on the quark structure of the meson, $C_F = 4/3$ is the color factor. The second function $T_H^2(x, Q^2, \mu_R^2)$ can be obtained from Eq. (2.7) using the replacement $x \leftrightarrow \bar{x}$

$$T_H^2(x, Q^2, \mu_R^2) = T_H^1(\bar{x}, Q^2, \bar{\mu}_R^2). \quad (2.9)$$

The hard-scattering amplitude $T_H(x, Q^2, \mu_R^2)$ must be symmetric under exchange $x \leftrightarrow \bar{x}$,

$$T_H(x, Q^2, \mu_R^2) = T_H(\bar{x}, Q^2, \bar{\mu}_R^2). \quad (2.10)$$

The replacement $x \leftrightarrow \bar{x}$, by means of which the function $T_H^2(x, Q^2, \mu_R^2)$ is found, in general, has to be applied also to the renormalization scale μ_R^2 changing it to $\bar{\mu}_R^2$. In the standard HSA one treats the μ_R^2 and $\bar{\mu}_R^2$ scales on the same footing by setting them equal, as a rule, to Q^2 . The choice $\mu_R^2 = \bar{\mu}_R^2 = Q^2$ satisfies both requirements (2.9) and (2.10) important for the hard-scattering amplitude. In the framework of the RC method the scales μ_R^2 and $\bar{\mu}_R^2$ have to be chosen in accordance with Eq. (2.6). Then the function $T_H^1(x, Q^2, \mu_R^2 = Q^2 x)$ takes the following form

$$T_H^1(x, Q^2) = \frac{N}{Q^2} \frac{1}{x} \left[1 + C_F \frac{\alpha_s(Q^2 x)}{4\pi} t(x) \right]. \quad (2.11)$$

The second part of the hard-scattering amplitude is given by the expression

$$T_H^2(x, Q^2) = \frac{N}{Q^2} \frac{1}{\bar{x}} \left[1 + C_F \frac{\alpha_s(Q^2 \bar{x})}{4\pi} t(\bar{x}) \right]. \quad (2.12)$$

One can see that within the RC method the requirements (2.9) and (2.10) hold as well.

In the framework of both the standard HSA and RC method the $M\gamma$ transition FF can be calculated employing the formula

$$\begin{aligned}
F_{M\gamma}(Q^2) &= T_H^1(x, Q^2) \otimes \phi_M(x, Q^2) + T_H^2(x, Q^2) \otimes \phi_M(x, Q^2) \\
&= T_H^1(x, Q^2) \otimes \phi_M(x, Q^2) + T_H^1(\bar{x}, Q^2) \otimes \phi_M(x, Q^2) \\
&= 2T_H^1(x, Q^2) \otimes \phi_M(x, Q^2).
\end{aligned} \tag{2.13}$$

In the last step we take into account that the DA of the pion is a symmetric $\phi_M(x, Q^2) = \phi_M(\bar{x}, Q^2)$ function.

The $M \equiv \pi^0, \eta, \eta'$ meson electromagnetic transition FF's were computed within the RC method in Refs. [5, 9]. In this work we generalize our approach by performing the computation of the $\pi^0\gamma$ transition FF in the context of the RC method, but employing instead of Eqs. (2.11) and (2.12) their versions symmetrized under $\mu_R^2 \leftrightarrow \bar{\mu}_R^2$ exchange, i.e.,

$$T_H^1(x, Q^2) = \frac{N}{Q^2} \frac{1}{x} \left\{ 1 + C_F \frac{1}{8\pi} [\alpha_s(Q^2 x) + \alpha_s(Q^2 \bar{x})] t(x) \right\}, \tag{2.14}$$

and

$$T_H^2(x, Q^2) = \frac{N}{Q^2} \frac{1}{\bar{x}} \left\{ 1 + C_F \frac{1}{8\pi} [\alpha_s(Q^2 x) + \alpha_s(Q^2 \bar{x})] t(\bar{x}) \right\}. \tag{2.15}$$

In the standard HSA Eqs. (2.14) and (2.15) coincide with Eq. (2.7) and its $x \leftrightarrow \bar{x}$ partner $T_H^2(x, Q^2, \mu_R^2 = Q^2)$, respectively. It is also not difficult to demonstrate that Eqs. (2.9), (2.10), and (2.13) hold for the hard-scattering amplitude determined by the new functions $T_H^1(x, Q^2)$ and $T_H^2(x, Q^2)$.

Here some comments concerning the symmetrization procedure are in order. To clarify this important point let us note that the virtual and real photons enter into the considering process (2.2) in an unequal manner. Indeed, the $M\gamma$ transition FF $F_{M\gamma}(Q^2)$ depends only on $Q^2 = -q_1^2$ ($q_2^2 = 0$). At the same time the virtual photon-meson,

$$\gamma^*(q_1) + \gamma^*(q_2) \rightarrow M(P),$$

transition FF $F_{M\gamma^*}(Q^2, \omega)$ is a function of the photon total virtuality Q^2 and asymmetry parameter ω (see the second paper of Ref. [16]),

$$Q^2 = Q_1^2 + Q_2^2, \quad \omega = \frac{Q_1^2}{Q^2}.$$

In the limits $\omega \rightarrow 0; 1$ the equality

$$F_{M\gamma^*}(Q^2, \omega = 0; 1) = F_{M\gamma}(Q^2)$$

must be valid. In order to meet this requirement and describe the real and virtual photon-meson transitions within the RC method in a unifying way, we adopt in this work Eqs. (2.14) and (2.15), because in the limits $\omega \rightarrow 0; 1$ the form factor $F_{M\gamma^*}(Q^2, \omega)$ found in the context of the RC method leads to $F_{M\gamma}(Q^2)$, computed by means namely of Eqs. (2.14) and (2.15). The symmetrization procedure, being discussed here, was used in Ref. [15] to calculate the

virtual and on-shell gluon- η' meson vertex function. In the present work we concentrate on the FF $F_{M\gamma}(Q^2)$, leaving the detailed analysis of $F_{M\gamma^*}(Q^2, \omega)$ for a future publication.

B. The pion distribution amplitude

Calculation of the FF $F_{\pi\gamma}(Q^2)$ requires the knowledge of the pion DA $\phi_\pi(x, Q^2)$, which is one of the key components in Eq. (2.3). It is known [17] that the pion DA can be expanded over the eigenfunctions of the one-loop Brodsky-Lepage equation, i.e., in terms of the Gegenbauer polynomials $\{C_n^{3/2}(2x-1)\}$,

$$\phi_\pi(x, Q^2) = \phi_{asy}(x) \left[1 + \sum_{n=2,4,\dots}^{\infty} b_n(Q^2) C_n^{3/2}(2x-1) \right], \quad (2.16)$$

where $\phi_{asy}(x)$ is the pion asymptotic DA,

$$\phi_{asy}(x) = \sqrt{3} f_\pi x(1-x), \quad (2.17)$$

with $f_\pi = 0.0923$ GeV being the pion decay constant.

The evolution of the DA on the factorization scale Q^2 is governed by the functions $b_n(Q^2)$,

$$b_n(Q^2) = b_n(\mu_0^2) \left[\frac{\alpha_s(Q^2)}{\alpha_s(\mu_0^2)} \right]^{\frac{\gamma_n}{\beta_0}}. \quad (2.18)$$

In Eq. (2.18) $\{\gamma_n\}$ are anomalous dimensions defined by the expression

$$\gamma_n = C_F \left[1 - \frac{2}{(n+1)(n+2)} + 4 \sum_{j=2}^{n+1} \frac{1}{j} \right]. \quad (2.19)$$

The constants $b_n(\mu_0^2) \equiv b_n^0$ are input parameters that form the shape of DA's and can be extracted from experimental data or obtained from the nonperturbative QCD computations at the normalization point μ_0^2 . The QCD coupling constant $\alpha_s(Q^2)$ at the two-loop approximation are given by the expression

$$\alpha_s(Q^2) = \frac{4\pi}{\beta_0 \ln(Q^2/\Lambda^2)} \left[1 - \frac{2\beta_1 \ln \ln(Q^2/\Lambda^2)}{\beta_0^2 \ln(Q^2/\Lambda^2)} \right]. \quad (2.20)$$

Here Λ is the QCD scale parameter, β_0 and β_1 are the QCD beta function one- and two-loop coefficients, respectively,

$$\beta_0 = 11 - \frac{2}{3}n_f, \quad \beta_1 = 51 - \frac{19}{3}n_f.$$

In the limit $Q^2 \rightarrow \infty$ all model DA's (2.16) reduce to the asymptotic form $\phi_{asy}(x)$. The nonasymptotic terms $\sim C_n^{3/2}(2x-1)$, $n \geq 2$ determine the deviation of the pion DA from the asymptotic form at moderate energy regimes and depend on the nonperturbative mesonic binding effects.

For the pion in the literature the various phenomenological DA's were proposed [6, 7, 17, 18, 19]. Thus, for example, in Ref. [18], employing the QCD sum rules method, the following pion DA was predicted

$$\phi(x, \mu_0^2) = \phi_{asy}(x) \left[1 + 0.758 C_2^{3/2}(2x-1) + 0.3942 C_4^{3/2}(2x-1) \right], \quad (2.21)$$

where the normalization point is $\mu_0 = 0.5 \text{ GeV}$.

The coefficients b_2^0 and b_4^0 were also extracted from the CLEO data on the $\pi^0\gamma$ transition FF in Ref. [7]. The authors used the QCD light-cone sum rules approach and included into their analysis the NLO perturbative and twist-four corrections. They found that in the model with two nonasymptotic terms, at the scale $\mu_0 = 2.4 \text{ GeV}$, the pion DA has the form

$$\phi(x, \mu_0^2) = \phi_{asy}(x) \left[1 + 0.19C_2^{3/2}(2x - 1) - 0.14C_4^{3/2}(2x - 1) \right]. \quad (2.22)$$

As is seen the pion DA's extracted from the experimental data depend on the used methods and on their accuracy. Although one claims that the meson DA is a process-independent quantity describing the internal structure of the meson itself, exploration of different exclusive processes with the same meson leads to a variety of DA's. This means that employed methods have shortcomings or do not encompass all mechanisms important for a given process. Such situation is pronounced in the case of the pion. The investigation carrying out in this work intends to improve the situation with the $\pi^0\gamma$ transition FF by taking into account at least one class of power corrections to the FF $F_{\pi\gamma}(Q^2)$.

To proceed it is convenient to expand the DA (2.16) over x and rewrite it in the following form:

$$\phi_\pi(x, Q^2) = \phi_{asy}(x) \sum_{n=0}^{\infty} K_n x^n, \quad (2.23)$$

where the sum runs over all n . The new coefficients K_n in the case of DA's with two nonasymptotic terms are given by the expressions

$$\begin{aligned} K_0 &= 1 + 6b_2(Q^2) + 15b_4(Q^2), \quad K_1 = -30[b_2(Q^2) + 7b_4(Q^2)], \\ K_2 &= 30[b_2(Q^2) + 28b_4(Q^2)], \quad K_3 = -60 \cdot 21b_4(Q^2), \quad K_4 = 30 \cdot 21b_4(Q^2). \end{aligned} \quad (2.24)$$

Here the functions $b_2(Q^2)$ and $b_4(Q^2)$ are defined by Eq. (2.18) with γ_2/β_0 and γ_4/β_0 being equal to

$$\frac{\gamma_2}{\beta_0} = \frac{50}{81}, \quad \frac{\gamma_4}{\beta_0} = \frac{364}{405}, \quad n_f = 3,$$

and

$$\frac{\gamma_2}{\beta_0} = \frac{2}{3}, \quad \frac{\gamma_4}{\beta_0} = \frac{364}{375}, \quad n_f = 4,$$

below and above the charm quark production threshold, respectively.

C. The $\pi^0\gamma$ transition FF within RC method

Computation of the photon-pion transition FF $F_{\pi\gamma}(Q^2)$ implies, naturally, integration over x in accordance with Eq. (2.13). Having inserted the explicit expression of the hard-scattering amplitude $T_H^1(x, Q^2)$ (2.14) and the pion DA (2.23) into Eq. (2.13) we encounter divergences, arising from the singularities of the coupling constant $\alpha_s(Q^2x)$ and $\alpha_s(Q^2\bar{x})$ in the limits $x \rightarrow 0; 1$. In the standard HSA this problem is solved by freezing the argument of the coupling constant and performing corresponding integrations with $\alpha_s(Q^2)$ [or $\alpha_s(Q^2/2)$]. In the RC method we allow the QCD coupling to run and therefore have to propose some method to cure these divergences.

As the first step we express the running coupling $\alpha_s(Q^2x)^1$, in terms of $\alpha_s(Q^2)$. This aim can be achieved by applying the renormalization-group equation to $\alpha_s(Q^2x)$ [20]. As a result we find

$$\alpha_s(Q^2x) \simeq \frac{\alpha_s(Q^2)}{1 + \ln x/t} \left[1 - \frac{\alpha_s(Q^2)\beta_1}{2\pi\beta_0} \frac{\ln[1 + \ln x/t]}{1 + \ln x/t} \right], \quad (2.25)$$

where $\alpha_s(Q^2)$ is the one-loop QCD coupling constant and $t = 4\pi/\beta_0\alpha_s(Q^2) = \ln(Q^2/\Lambda^2)$. Equation (2.25) expresses $\alpha_s(Q^2x)$ in terms of $\alpha_s(Q^2)$ with an $\sim \alpha_s^2(Q^2)$ order accuracy.

Inserting Eq. (2.25) into the formula for the transition FF Eq. (2.13), we obtain integrals, which are still divergent, but can be calculated using existing methods. One of them (see for details Ref. [11]) allows one to obtain the form factor as a perturbative series in $\alpha_s(Q^2)$ with factorially growing coefficients $C_n \sim (n-1)!$,

$$Q^2 F_{\pi\gamma}(Q^2) \sim \sum_{n=1}^{\infty} \left[\frac{\alpha_s(Q^2)}{4\pi} \right]^n \beta_0^{n-1} C_n. \quad (2.26)$$

But, it is known that a perturbative QCD series with factorially growing coefficients is a signal for the IR renormalon nature of the divergences in Eq. (2.26). The convergence radius of such series is zero and its resummation should be performed by employing the Borel integral technique. Namely, one has to determine the Borel transform $B[Q^2 F_{\pi\gamma}](u)$ of the corresponding series [21]

$$B[Q^2 F_{\pi\gamma}](u) = \sum_{n=1}^{\infty} \frac{u^{n-1}}{(n-1)!} C_n, \quad (2.27)$$

and in order to define the sum Eq. (2.26), or to find the resummed expression for the form factor, one has to invert $B[Q^2 F_{\pi\gamma}](u)$ to get

$$[Q^2 F_{\pi\gamma}(Q^2)]^{res} \sim \text{P.V.} \int_0^{\infty} du \exp\left[-\frac{4\pi u}{\beta_0\alpha_s(Q^2)}\right] B[Q^2 F_{\pi\gamma}](u). \quad (2.28)$$

Because the coefficients of the series Eq. (2.26) behave like $C_n \sim (n-1)!$, the Borel transform (2.27) contains poles located at the positive u axis of the Borel plane, which are exactly the IR renormalon poles. Therefore the inverse Borel transformation (2.28) can be computed only after regularization of these pole singularities. One of the methods of such regularization, adopted also in the present work, is the principal value prescription. In other words, the IR renormalon divergences in Eq. (2.28) have to be removed by computing the integral in the sense of the Cauchy principal value. Only after this regularization the inverse Borel transformation defines the resummed FF.

Fortunately, these intermediate operations can be omitted with the help of the following operations. Namely, let us introduce the inverse Laplace transformations of the functions in Eq. (2.25), i.e.,

$$\frac{1}{(t+z)^\nu} = \frac{1}{\Gamma(\nu)} \int_0^{\infty} du \exp[-u(t+z)] u^{\nu-1}, \quad \text{Re}\nu > 0, \quad (2.29)$$

and

¹ Similar consideration is valid also for the running coupling $\alpha_s(Q^2\bar{x})$.

$$\frac{\ln[t+z]}{(t+z)^2} = \int_0^\infty du \exp[-u(t+z)](1 - \gamma_E - \ln u)u, \quad (2.30)$$

where $\Gamma(z)$ is the Gamma function, $\gamma_E \simeq 0.577216$ is the Euler constant, and $z = \ln x$ [or $z = \ln \bar{x}$ in the case of $\alpha_s(Q^2\bar{x})$]. Then, using Eqs. (2.29) and (2.30) for the QCD coupling $\alpha_s(Q^2x)$ we find [9, 15]

$$\alpha_s(Q^2x) = \frac{4\pi}{\beta_0} \int_0^\infty du e^{-ut} R(u, t) x^{-u}, \quad (2.31)$$

where the function $R(u, t)$ is defined as

$$R(u, t) = 1 - \frac{2\beta_1}{\beta_0^2} u(1 - \gamma_E - \ln t - \ln u). \quad (2.32)$$

Having used Eq. (2.31) and performed integration over x , for the scaled $\pi^0\gamma$ transition FF we get

$$Q^2 F_{\pi\gamma}(Q^2) = \sqrt{3} f_\pi N \left\{ \sum_{n=0}^\infty \frac{K_n}{n+1} + \frac{4}{3\beta_0} \int_0^\infty du e^{-ut} R(u, t) \right. \\ \left. \times \sum_{n=0}^\infty K_n [A_n(u) + \tilde{A}_n(u)] \right\}. \quad (2.33)$$

Here the term $\sim A_n(u)$ appears in the result of the integration of the second term in Eq. (2.14), whereas the term $\sim \tilde{A}_n(u)$ owing to the third term in Eq. (2.14). The functions $A_n(u)$ and $\tilde{A}_n(u)$ have the following forms:

$$A_n(u) = \frac{d^2}{d\beta^2} B(2, \beta)|_{\beta=n+1-u} - \frac{d}{d\beta} B(1, \beta)|_{\beta=n+2-u} - 9B(2, n+1-u) \\ = \frac{2}{(n+1-u)^3} - \frac{2}{(n+2-u)^3} + \frac{1}{(n+2-u)^2} - \frac{9}{(n+1-u)(n+2-u)}, \quad (2.34)$$

and

$$\tilde{A}_n(u) = \frac{\partial^2}{\partial\beta^2} B(2-u, \beta)|_{\beta=n+1} - \frac{\partial}{\partial\beta} B(1-u, \beta)|_{\beta=n+2} - 9B(2-u, n+1) \\ = B(n+1, 2-u) [(\psi(n+1) - \psi(n+3-u))^2 + \psi'(n+1) - \psi'(n+3-u)] \\ - B(n+2, 1-u) [\psi(n+2) - \psi(n+3-u)] - 9B(2-u, n+1), \quad (2.35)$$

where $B(x, y)$ is the beta function $B(x, y) = \Gamma(x)\Gamma(y)/\Gamma(x+y)$ and $\psi(z) = d[\ln \Gamma(z)]/dz$.

The functions $A_n(u)$ and $\tilde{A}_n(u)$ contain the poles on the positive real axis of the plane u . Indeed, the function $A_n(u)$ has the finite number of triple, double, and single poles located at the points $u_0 = n+2$ and triple and single ones at $u_0 = n+1$. In order to reveal the pole structure of the function $\tilde{A}_n(u)$, it is convenient to use the following formulas [23]

$$\psi(z) = -\gamma_E + (z-1) \sum_{k=0}^\infty \frac{1}{(k+1)(k+z)}, \quad \psi'(z) = \sum_{k=0}^\infty \frac{1}{(k+z)^2}. \quad (2.36)$$

Here we write down, as an example, the function $\tilde{A}_0(u)$, which after some manipulations takes the form

$$\begin{aligned} \tilde{A}_0(u) = & (2-u) \left[\sum_{k=0}^{\infty} \frac{1}{(k+1)(k+3-u)} \right]^2 - \frac{1}{2-u} \sum_{k=0}^{\infty} \frac{1}{(k+3-u)^2} \\ & + \frac{1}{1-u} \sum_{k=0}^{\infty} \frac{1}{(k+1)(k+3-u)} - \frac{1}{1-u} + \frac{\psi'(1) - 8}{2-u}. \end{aligned} \quad (2.37)$$

Now it is clear that $\tilde{A}_0(u)$ contains the infinite number of the double poles located at $u_0 = k + 3$ and the single ones at $u_0 = 1, 2, k + 3$. The similar analysis can be fulfilled for $\tilde{A}_n(u)$, $n > 0$ as well. Hence by employing Eq. (2.31) we have transformed the endpoint $x \rightarrow 0; 1$ divergences in Eq. (2.13) into the IR renormalon pole divergences in Eq. (2.33). The integral in Eq. (2.33) is the inverse Borel transformation (2.28), where the Borel transform $B[Q^2 F_{\pi\gamma}](u)$ of the NLO part of the scaled FF is defined (up to constant factor) as

$$B[Q^2 F_{\pi\gamma}](u) \sim R(u, t) \sum_{n=0}^{\infty} K_n [A_n(u) + \tilde{A}_n(u)]. \quad (2.38)$$

The IR renormalon divergences in Eq. (2.33) must be removed by means of the the principal value prescription. The inverse Borel transformation after such regularization, as we have just pointed out above, becomes the resummed form factor $[Q^2 F_{\pi\gamma}(Q^2)]^{res}$. Therefore all integrals over u hereafter have to be understood in the sense of the Cauchy principal value.

The expression $[Q^2 F_{\pi\gamma}(Q^2)]^{res}$ contains the power-suppressed corrections $\sim 1/Q^{2n}$, $n = 1, 2, \dots$ to the scaled FF, implicitly existing in the QCD factorization formula (2.3). The detailed discussion of relevant problems can be found in Refs. [9, 15]. Here, for completeness, we outline the important points of this analysis. To make the discussion of this question as transparent as possible, let us for a moment neglect the nonleading term $\sim \alpha_s^2(Q^2)$ in Eq. (2.25) and consequently make the replacement $R(u, t) \rightarrow 1$ in Eq. (2.31). Then the integrals in the scaled and resummed FF with multiple IR renormalon poles at $u_0 = n$ can be easily expressed in terms of the integrals with a single IR renormalon pole at the same point [see Eqs. (3.6) and (3.15)], so that our formula (2.33) will consist of some linear combinations of the integrals,

$$\frac{4\pi}{\beta_0} \int_0^{\infty} \frac{e^{-ut} du}{n-u} = \frac{1}{n} f_{2n}(Q), \quad (2.39)$$

where $f_{2n}(Q)$ are the moment integrals,

$$f_p(Q) = \frac{p}{Q^p} \int_0^Q dk k^{p-1} \alpha_s(k^2). \quad (2.40)$$

The integrals $f_p(Q)$ were calculated in Ref. [22] using the IR matching scheme:

$$f_p(Q) = \left(\frac{\mu_I}{Q} \right)^p f_p(\mu_I) + \alpha_s(Q^2) \sum_{n=0}^N \left[\frac{\beta_0}{2\pi p} \alpha_s(Q^2) \right]^n [n! - \Gamma(n+1, p \ln(Q/\mu_I))], \quad (2.41)$$

where μ_I is the infrared matching scale and $\Gamma(n+1, z)$ is the incomplete Gamma function. In Eq. (2.41) $\{f_p(\mu_I)\}$ are phenomenological parameters, which represent the weighted average

of $\alpha_s(k^2)$ over the IR region $0 < k < \mu_I$ and act at the same time as infrared regulators of the right-hand side (RHS) of Eq. (2.39). The first term on the right-hand side of Eq. (2.41) is the power-suppressed contribution to $f_p(Q)$ and models the "soft" part of the moment integral. It cannot be calculated within the perturbative QCD, whereas the second term on the RHS of Eq. (2.41) is the perturbatively calculable part of the function $f_p(Q)$, representing its hard perturbative "tail." In other words, the IR matching scheme allows one to estimate power corrections to the moment integrals by explicitly dissecting them out from the full expression, and introducing new nonperturbative parameters $f_p(\mu_I)$. The same moment integrals $f_p(Q)$ computed in the framework of the RC method [LHS of Eq. (2.39)], contain information on both their soft and the perturbative components. Therefore we can state that the scaled and resummed FF (2.33) contain power corrections $\sim 1/Q^{2n}$. In phenomenological applications both the IR matching scheme and the RC method can be employed. But the RC method has an advantage over the IR matching scheme, because it allows one to compute the functions $f_p(Q)$ without introducing the new nonperturbative parameters μ_I and $f_p(\mu_I)$. Moreover, using this method, the parameters $f_p(\mu_I)$ themselves can be calculated in good agreement with model calculations and available experimental data [15, 24].

But the principal value prescription itself generates in the each integral over u higher-twist ambiguities,

$$\sim \sum_q N_q \frac{\Phi_q(Q^2)}{Q^{2q}},$$

where $\Phi_q(Q^2)$ is a calculable function fixed by the residue of the integral at the pole $u_0 = q$ and N_q is some numerical constant. The ambiguities taken into account in Eq. (2.33) modify the Borel resummed $\pi^0\gamma$ transition FF, yielding

$$[Q^2 F_{\pi\gamma}(Q^2)]^{res} \rightarrow [Q^2 F_{\pi\gamma}(Q^2)]^{res} + [Q^2 F_{\pi\gamma}(Q^2)]^{HT}. \quad (2.42)$$

The HT term depends on the known functions $\{\Phi_q(Q^2)\}$ and coefficients $\{K_q\}$ and on the unknown numerical constants $\{N_q\}$. In accordance with the "ultraviolet dominance assumption" this HT ambiguity allows one to estimate higher-twist corrections to the scaled form factor $Q^2 F_{\pi\gamma}(Q^2)$ coming from sources another than end-point integration. By fitting the constants $\{N_q\}$ to experimental data one can deduce some information concerning the magnitude of such corrections.

III. ASYMPTOTIC LIMIT OF THE RESUMMED $\pi^0\gamma$ TRANSITION FF

As we have emphasized above, the resummed $\pi^0\gamma$ transition FF contains the power corrections appearing due to the end-point integration. These corrections in the region of a moderate momentum transfer Q^2 are essential for explaining the experimental data [5, 9, 12, 13]. But it is also evident that in the asymptotic limit $Q^2 \rightarrow \infty$, where all higher-twist corrections should vanish, the standard HSA with frozen $\alpha_s(Q^2)$ and the pion asymptotic DA $\phi_{asy}(x)$ leads to the correct expression for the $\pi^0\gamma$ transition FF. Consequently, in the limit $Q^2 \rightarrow \infty$ from the resummed FF we have to regain the asymptotic one.

In the limit $Q^2 \rightarrow \infty$ the pion DA goes to its asymptotic form, i.e.,

$$\phi_\pi(x, Q^2) \xrightarrow{Q^2 \rightarrow \infty} \phi_{asy}(x), \quad (3.1)$$

which in the terms of the coefficients K_n means

$$K_0 \rightarrow 1, \quad K_n \rightarrow 0, \quad n > 0. \quad (3.2)$$

We take also into account that in this limit the subleading term in the expansion of $\alpha_s(Q^2 x)$ through $\alpha_s(Q^2)$ has to be neglected. In other words, in the limit $Q^2 \rightarrow \infty$ we have to fulfill the replacement

$$\int_0^\infty du e^{-ut} R(u, t) \xrightarrow{Q^2 \rightarrow \infty} \int_0^\infty du e^{-ut}. \quad (3.3)$$

After these operations the resummed FF takes the following form:

$$[Q^2 F_{\pi\gamma}(Q^2)]^{res} \xrightarrow{Q^2 \rightarrow \infty} \sqrt{3} f_\pi N \left\{ 1 + \frac{4}{3\beta_0} \int_0^\infty du e^{-ut} [A_0(u) + \tilde{A}_0(u)] \right\}. \quad (3.4)$$

But Eq. (3.4) is not the final expression, because in the integral above $t = \ln(Q^2/\Lambda^2)$ and its $Q^2 \rightarrow \infty$ limit still has to be computed.

To this end, we start from the simple case and consider the integral

$$I_1 = \int_0^\infty du e^{-ut} A_0(u) = \int_0^\infty du e^{-ut} \left[\frac{2}{(1-u)^3} - \frac{2}{(2-u)^3} + \frac{1}{(2-u)^2} - \frac{9}{1-u} + \frac{9}{2-u} \right]. \quad (3.5)$$

The integrals in Eq. (3.5) with the triple and double poles can be reduced to ones with single poles:

$$\begin{aligned} \int_0^\infty \frac{e^{-ut} du}{(n-u)^3} &= -\frac{1}{2n^2} - \frac{\ln \lambda}{2n} + \frac{\ln^2 \lambda}{2} \frac{li(\lambda^n)}{\lambda^n}, \\ \int_0^\infty \frac{e^{-ut} du}{(n-u)^2} &= -\frac{1}{n} + \ln \lambda \frac{li(\lambda^n)}{\lambda^n}, \quad \int_0^\infty \frac{e^{-ut} du}{n-u} = \frac{li(\lambda^n)}{\lambda^n}, \end{aligned} \quad (3.6)$$

where the first two equalities are obtained performing integrations by parts. Here the logarithmic integral $li(\zeta)$ is defined as

$$li(\zeta) = \text{P.V.} \int_0^\zeta \frac{dt}{\ln t}, \quad (3.7)$$

and $\lambda = Q^2/\Lambda^2$. Now using the expansion of $li(\zeta^n)/\zeta^n$ in inverse powers of $\ln \zeta$ [15],

$$\frac{li(\zeta^n)}{\zeta^n} \simeq \frac{1}{n \ln \zeta} \sum_{m=0}^M \frac{m!}{(n \ln \zeta)^m}, \quad M \gg 1, \quad (3.8)$$

and keeping in the expressions

$$\ln^2 \lambda \frac{li(\lambda^n)}{\lambda^n}, \quad \ln \lambda \frac{li(\lambda^n)}{\lambda^n},$$

terms up to $O(1/\ln \lambda)$ order, we get

$$I_1 \xrightarrow{Q^2 \rightarrow \infty} -\frac{5}{2} \frac{1}{\ln \lambda}. \quad (3.9)$$

The situation with the second integral,

$$I_2 = \int_0^\infty du e^{-ut} \tilde{A}_0(u), \quad (3.10)$$

is more subtle. In this case, instead of using the explicit form of $\tilde{A}_0(u)$, we consider the integral

$$I_2 = \int_0^\infty du e^{-ut} \int_0^1 dx \bar{x}^{1-u} t(x) = \int_0^\infty du e^{-ut} \int_0^1 dx x^{1-u} t(\bar{x}), \quad (3.11)$$

from which Eq. (3.10) has been derived. We are going to explain our technique, analyzing one of the components of the function $t(\bar{x})$. Namely, let us calculate the $Q^2 \rightarrow \infty$ limit of the integral

$$I_2^1 = \int_0^\infty du e^{-ut} \int_0^1 dx x^{1-u} \ln^2(1-x). \quad (3.12)$$

Having expanded $\ln^2(1-x)$ in powers of x ,

$$\ln^2(1-x) = 2 \sum_{k=1}^{\infty} \frac{1}{k+1} [\psi(k+1) - \psi(1)] x^{k+1}, \quad (3.13)$$

we obtain

$$\int_0^1 dx x^{1-u} \ln^2(1-x) = 2 \sum_{k=1}^{\infty} \frac{1}{k+1} [\psi(k+1) - \psi(1)] \frac{1}{k+3-u}. \quad (3.14)$$

Substituting Eq. (3.14) into the integral I_2^1 ,

$$2 \sum_{k=1}^{\infty} \frac{1}{k+1} [\psi(k+1) - \psi(1)] \int_0^\infty \frac{du e^{-ut}}{k+3-u} = 2 \sum_{k=1}^{\infty} \frac{1}{k+1} [\psi(k+1) - \psi(1)] \frac{\text{li}(\lambda^{k+3})}{\lambda^{k+3}}, \quad (3.15)$$

and using the leading order term in expansion (3.8), in the limit $Q^2 \rightarrow \infty$ we get

$$I_2^1 \xrightarrow{Q^2 \rightarrow \infty} 2 \sum_{k=1}^{\infty} \frac{1}{k+1} [\psi(k+1) - \psi(1)] \frac{1}{k+3} \frac{1}{\ln \lambda}. \quad (3.16)$$

Now, having repeated the described above operations in the reverse order, it is easy to see that

$$2 \sum_{k=1}^{\infty} \frac{1}{k+1} [\psi(k+1) - \psi(1)] \frac{1}{k+3} \frac{1}{\ln \lambda} = \frac{1}{\ln \lambda} \int_0^1 dx x \ln^2(1-x). \quad (3.17)$$

In other words, the asymptotic limit $Q^2 \rightarrow \infty$ transforms the integral I_2^1 in accordance with the rule

$$I_2^1 \xrightarrow{Q^2 \rightarrow \infty} \frac{1}{\ln \lambda} \int_0^1 dx x \ln^2(1-x). \quad (3.18)$$

The same conclusion is valid also for the other terms from Eq. (2.8). Summing up, we derive the limit of the integral I_2 ,

$$\begin{aligned} I_2 \xrightarrow{Q^2 \rightarrow \infty} \frac{1}{\ln \lambda} \int_0^1 dx x t(1-x) &= \frac{1}{\ln \lambda} B(1,2) \left\{ [(\psi(1) - \psi(3))^2 + \psi'(1) - \psi'(3)] \right. \\ &\quad \left. - [\psi(2) - \psi(3)] - 9 \right\}. \end{aligned} \quad (3.19)$$

The expression (3.19) without the factor $1/\ln \lambda$ is nothing more than $\tilde{A}_0(u)$ at $u = 0$. The following operations are trivial and lead to

$$I_2 \xrightarrow{Q^2 \rightarrow \infty} -\frac{5}{2} \frac{1}{\ln \lambda}. \quad (3.20)$$

As is seen, both the functions I_1 and I_2 have the same limits. Consequently, for the resummed FF we find

$$[Q^2 F_{\pi\gamma}(Q^2)]^{res} \xrightarrow{Q^2 \rightarrow \infty} 2f_\pi \left[1 - \frac{5}{3\pi} \alpha_s(Q^2) \right], \quad (3.21)$$

in deriving of which the value of the constant N ,

$$N = \sqrt{12}(e_u^2 - e_d^2) \quad (3.22)$$

for the pion has been utilized. Equation (3.21) can be readily obtained within the standard HSA employing the pion asymptotic DA. Our analysis proves that in the asymptotic limit the Borel resummed FF leads to the correct expression (3.21), which we consider as one of justifications of the symmetrization procedure. It is also worth remarking that the "old" version of the hard-scattering amplitude $T_H(x, Q^2)$ [see Eqs. (2.11) and (2.12)] gives the correct asymptotic FF as well, that is evident from Eq. (3.9). Hence in the asymptotic limit both the ordinary and symmetrized RC methods describe correctly the $\pi^0\gamma$ transition FF, the difference between them being sizeable at the moderate values of the momentum transfer, $Q^2 \sim$ a few GeV^2 .

IV. EXTRACTING THE PION DA FROM THE CLEO DATA

In this section we present the pion phenomenological DA's extracted from the CLEO data within the SRC method. In our calculations below we shall use the following values of the parameters Λ and μ_0

$$\Lambda_4 = 0.25 \text{ GeV}, \quad \mu_0^2 = 1 \text{ GeV}^2. \quad (4.1)$$

As is known (see for review Ref. [25]), the IR renormalon calculus can be applied for the estimation of power corrections to some physical quantity in the region of the high momentum transfers $Q^2 \gg \Lambda^2$. Our choice for the parameters (4.1) leads to the requirement $16 Q^2 \gg 1$. Because the recent CLEO data [4] on the $\pi^0\gamma$ transition FF lie in the domain $1.64 \text{ GeV}^2 \leq Q^2 < 10 \text{ GeV}^2$, we include them into our numerical analysis to deduce the pion model DA's. Namely at these moderate momentum transfers the power corrections play the important role, modifying both quantitatively and qualitatively predictions for $Q^2 F_{\pi\gamma}(Q^2)$ obtained within the standard HSA.

The Borel resummed $\pi^0\gamma$ transition FF implies summations over n and k , the latter arising from $\sim \tilde{A}_n(u)$ terms. The summation over n does not create problems, because in our studies we use the pion asymptotic and model DA's with one and two nonasymptotic terms. Therefore the maximal value of n in the sum is $N_{\max} = 0$ and $2, 4$, respectively. It is worth noting that Eq. (2.33) is a general expression valid for the pion DA's with an arbitrary number of nonasymptotic terms. The next terms $\sim C_n(2x-1)$, $n > 4$ can be easily included into our scheme by modifying only expressions of the coefficients K_n and N_{\max} . Contrary to the case with n , at fixed n summation over k runs from $k = 0$ to $k = \infty$ and has to be truncated at some k_{\max} . In other words, the results of numerical computations depend on k_{\max} . In order to check their sensitivity to a chosen value of k_{\max} , we have performed calculation of the FF with $k_{\max} = 50$ and $k_{\max} = 100$. We have found that for the pion asymptotic DA the ratio

$$R(Q^2) = \frac{[Q^2 F_{\pi\gamma}(Q^2)]^{res}(k_{\max} = 100)}{[Q^2 F_{\pi\gamma}(Q^2)]^{res}(k_{\max} = 50)} \quad (4.2)$$

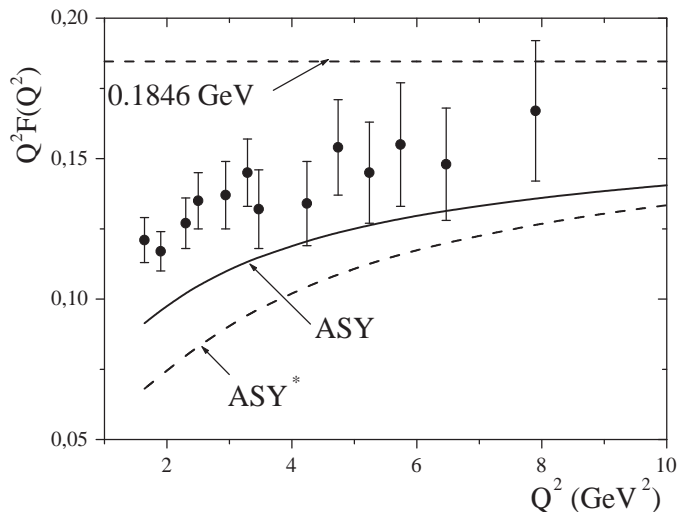


FIG. 1: The scaled and resummed $\pi^0\gamma$ transition form factor $Q^2 F_{\pi\gamma}(Q^2)$ as a function of Q^2 . The curves ASY and ASY* are computed using the pion asymptotic DA (2.17). The curve ASY* corresponds to the FF obtained within the ordinary RC approach, whereas for calculation of the curve ASY the SRC method is employed. The upper dashed line shows the model-independent $Q^2 \rightarrow \infty$ limit for the FF. The data are borrowed from Ref. [4].

at $Q^2 = 1 \text{ GeV}^2$ is equal to $R(1 \text{ GeV}^2) = 1.0027$ and to $R(10 \text{ GeV}^2) = 1.0011$ at $Q^2 = 10 \text{ GeV}^2$. We have obtained a similar picture employing the pion various model DA's. Since the correction to $Q^2 F_{\pi\gamma}(Q^2)$ originating from the next $k = 51 - 100$ terms does not exceed $3 \cdot 10^{-3}$ of those from the first $k = 0 - 50$ ones, in numerical computations we set $k_{\text{max}} = 50$. Such output is understandable, because in the resummed FF dominate contributions from the nearest to $u = 0$ IR renormalon poles.

We start our analysis of the $\pi^0\gamma$ transition FF from the pion asymptotic DA in order to reveal the impact of the symmetrization procedure on the predictions, as well as to find out how large is the deviation of these predictions from the data points. Our results are shown in Fig. 1. As is seen, the scaled and resummed FF $Q^2 F_{\pi\gamma}(Q^2)$ computed using the SRC method in the region of the momentum transfers $1.64 \text{ GeV}^2 \leq Q^2 \leq 5 \text{ GeV}^2$ are considerably larger than the one obtained by means of the ordinary RC approach. As a result, the deviation of the curve ASY from the data points are smaller than that of ASY*. Nevertheless, such deviation exists and some admixture of nonasymptotic terms in the pion DA is needed to explain the data.

In Fig. 2 we depict (the shaded area) the 1σ area for values of the input parameters b_2^0, b_4^0 in the $b_4^0 - b_2^0$ plane. This means that the $\pi^0\gamma$ transition FF computed in the context of the SRC method employing the pion model DA's with Gegenbauer coefficients belonging to the shaded region describes the CLEO data with a 1σ accuracy.

In Fig. 3 we plot the 1σ area for the $\pi^0\gamma$ transition FF itself. The central curves with $b_2^0 = 0.16, b_4^0 = 0$ (the DA's with one nonasymptotic term) and $b_2^0 = 0.25, b_4^0 = -0.05$ (the DA's with two nonasymptotic terms) are also shown. One sees that the shapes of the curves with $b_4^0 = 0$ and $b_4^0 < 0$ differ from each other. Indeed, the curves with $b_4^0 < 0$ are sharper

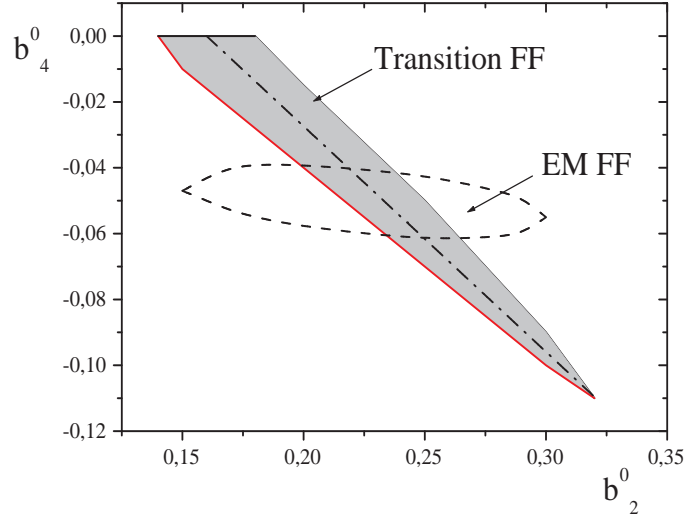


FIG. 2: The 1σ areas in the $b_4^0 - b_2^0$ plane of the input parameters. The shaded area is found from analysis of the CLEO data on the $\pi^0\gamma$ transition FF. The region bounded by the dashed lines is extracted from the data on the pion electromagnetic (EM) FF. The dot-dashed line is the diagonal determined by Eq. (4.4).

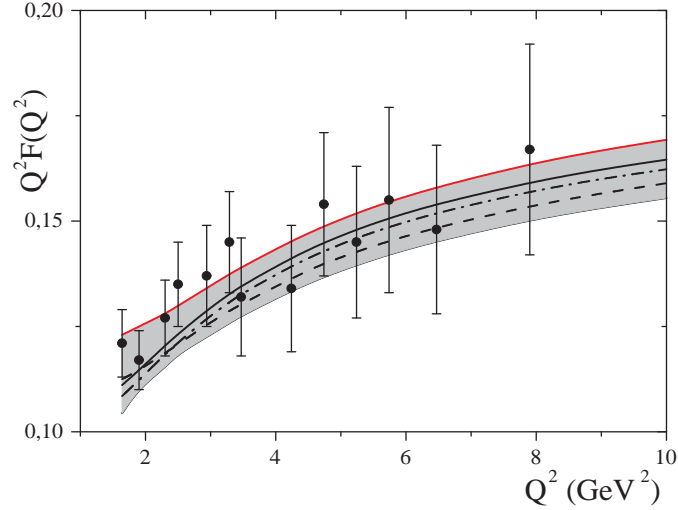


FIG. 3: The scaled and resummed $\pi^0\gamma$ transition FF vs Q^2 . The shaded area demonstrates 1σ region for the FF. Correspondence between the curves and the input parameters is; for the solid line $b_2^0 = 0.25$, $b_4^0 = -0.05$; for the dashed line $b_2^0 = 0.16$, $b_4^0 = 0$; and for the dot-dashed line $b_2^0 = 0.23$, $b_4^0 = -0.05$.

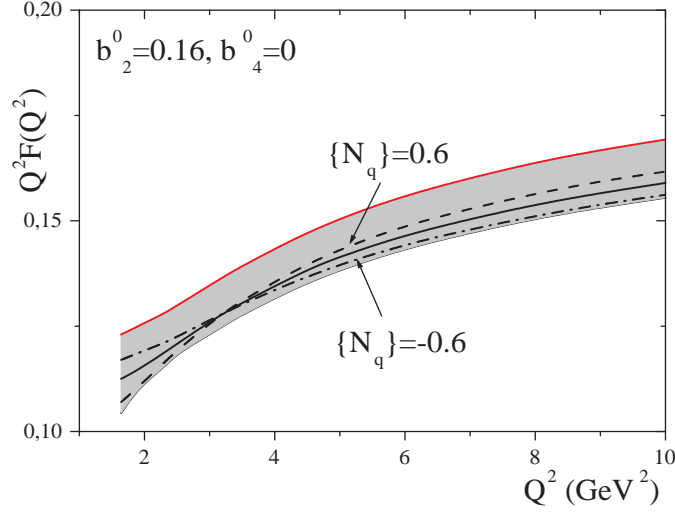


FIG. 4: The scaled and resummed form factor $Q^2 F_{\pi\gamma}(Q^2)$ with and without HT ambiguities. The solid line describes FF without HT ambiguities. The broken lines are found employing Eq. (2.42) and numerical constants $\{N_q\}$ shown in the figure.

relative to ones with $b_4^0 = 0$. Therefore the boundaries of the 1σ area are determined by superposition of curves of these two types. Our analysis in the case of the DA's with one nonasymptotic term leads to the following estimation

$$b_2^0 = 0.16 \pm 0.02, \quad b_4^0 = 0. \quad (4.3)$$

In the case of DA's with two nonasymptotic terms allowed value of b_2^0, b_4^0 cover the shaded area in Fig. 2. Below we write down sample values of the parameters,

$$\begin{aligned} b_2^0 &= 0.2, & b_4^0 &\in [-0.02, -0.04], \\ b_2^0 &= 0.25, & b_4^0 &\in [-0.05, -0.07], \end{aligned}$$

and

$$b_2^0 = 0.3, \quad b_4^0 \in [-0.09, -0.1].$$

The "diagonal" of the 1σ area is determined by the expression

$$b_2^0 + 1.46b_4^0 = 0.16, \quad b_4^0 \in [0, -0.11] \quad (4.4)$$

and is shown in Fig. 2 by the dot-dashed line.

As we have noted above, the principal value prescription generates HT ambiguities that in conjunction with the "ultraviolet dominance assumption" can be used to estimate HT corrections to the form factor originating from another source (for example, from the pion HT DA's). We have performed relevant computations, as a sample, for the pion DA with one nonasymptotic term $b_2^0(1 \text{ GeV}^2) = 0.16$ and $\{N_q\} = \pm 0.6$, $q = 1, 2, \dots, 50$ (Fig. 4). We find that the values $\{N_q\} = \pm 0.6$ determine the upper and lower bounds for the constants $\{N_q\}$ in order that FF remain within the 1σ region. The $\pi^0\gamma$ transition FF with HT ambiguities

corresponding to $\{N_q\} = -0.6$ ($\{N_q\} = 0.6$) at $Q^2 < 3.5 \text{ GeV}^2$ is larger (smaller) than the FF without such corrections and are smaller (larger) for $Q^2 > 3.5 \text{ GeV}^2$. The HT ambiguities, obeying the "1 σ constraint" do not exceed the level $\sim \pm 5\%$ of the transition FF at the momentum transfers $Q^2 = 1.64 - 2 \text{ GeV}^2$ and reach only $\sim \mp 1.8\%$ at $Q^2 = 9 - 10 \text{ GeV}^2$.

V. THE ELECTROMAGNETIC FORM FACTOR $F_\pi(Q^2)$

In this section we compute the pion electromagnetic FF $F_\pi(Q^2)$ in the framework of the RC method in order to extract further constraints on the parameters b_2^0, b_4^0 .

The FF $F_\pi(Q^2)$ is the important quantity characterizing the pion, which was thoroughly investigated in the context of PQCD [24, 26, 27]. It was also studied in various experiments [28, 29]. Within the RC method FF's $F_M(Q^2)$ of the light mesons $M = \pi, K, \rho_L$ were considered in Refs. [11, 12, 13, 24]. Therefore below we outline only main stages of the RC analysis of the FF $F_M(Q^2)$.

In the standard HSA the FF $F_\pi(Q^2)$ is given by the factorization formula

$$F_\pi(Q^2) = \int_0^1 dx \int_0^1 dy \phi_\pi^*(y, Q^2) T_H(x, y, Q^2) \phi_\pi(x, Q^2). \quad (5.1)$$

Here $T_H(x, y, Q^2)$ is the hard-scattering amplitude of the subprocess $q\bar{q}' + \gamma^* \rightarrow q\bar{q}'$, $Q^2 = -q^2$ is the momentum transfer, q being the four-momentum of the virtual photon. In Eq. (5.1) the factorization scale from the very beginning is chosen equal to $\mu_F^2 = Q^2$.

At the leading order of PQCD the amplitude $T_H(x, y, Q^2)$ has the form

$$T_H(x, y, Q^2) = \frac{16\pi C_F}{Q^2} \left[\frac{2}{3} \frac{\alpha(\bar{\mu}_R^2)}{\bar{x}\bar{y}} + \frac{1}{3} \frac{\alpha(\mu_R^2)}{xy} \right]. \quad (5.2)$$

In accordance with the ideology of the RC method the argument of the QCD coupling in Eq. (5.2) has to be chosen as

$$\mu_R^2 = xyQ^2, \quad \bar{\mu}_R^2 = \bar{x}\bar{y}Q^2. \quad (5.3)$$

Such choice allows one to get rid of terms $\sim \ln(\bar{x}\bar{y}Q^2/\bar{\mu}_R^2), \ln(xyQ^2/\mu_R^2)$ appearing in the amplitude $T_H(x, y, Q^2)$ at the next-to-leading order of PQCD and minimizes the higher-order corrections to $F_\pi(Q^2)$. We can also adopt the scheme

$$\mu_R^2 = xQ^2, \quad \bar{\mu}_R^2 = \bar{x}Q^2, \quad (5.4)$$

obtained from Eq. (5.3) by freezing y . In the framework of the standard HSA one freezes both of x, y and compute the form factor with $\mu_R^2 = \bar{\mu}_R^2 = Q^2$ (or $Q^2/4$) [26].

In the above we have chosen x as the running variable. Alternatively, we can fix x and choose y as the running one or to compute the mean value of the sum of the FF's calculated using both possibilities; due to the symmetry of $T_H(x, y, Q^2)$ and Eq. (5.1) itself with respect to x, y we will get the same result. Of course, the second option (5.4) leaves in the NLO correction some logarithmic terms, but it leads to better agreement with the experimental data than the choice (5.3) [13]. Therefore in our computations we use the option (5.4). Since in the considering process the partonic hard subprocess contains only one external virtual photon, we do not perform the symmetrization of the hard-scattering amplitude. Stated

differently, below we write down the expression $[Q^2 F_\pi(Q^2)]^{res}$, obtained in the framework of the ordinary RC method.

The Borel resummed pion electromagnetic FF are determined by the formula [13]

$$[Q^2 F_\pi(Q^2)]^{res} = \frac{(16\pi f_\pi)^2}{\beta_0} \sum_{l=0}^{\infty} K_l B(2+l, 1) \times \sum_{n=0}^{\infty} K_n \int_0^{\infty} du e^{-ut} R(u, t) B(2+n, 1-u). \quad (5.5)$$

The integrand in Eq. (5.5) has a finite number of the single IR renormalon poles. In fact, the sums in the general expression (5.5) in practice run up to some L_{\max} , N_{\max} , which for DA's with two nonasymptotic terms are $L_{\max} = N_{\max} = 4$. The maximum number of IR renormalon poles results from the term $\sim B(6, 1-u)$. The latter can be rewritten in the following way

$$B(6, 1-u) = \frac{\Gamma(6)\Gamma(1-u)}{\Gamma(7-u)} = \frac{120}{(1-u)(2-u)\dots(6-u)},$$

making our statement evident. It is implied that the pole divergences are removed by the principal value prescription.

In the asymptotic limit $Q^2 \rightarrow \infty$ from the resummed FF we recover the standard HSA expression. In fact, acting along the line described in the detailed form in Sec. III, we get

$$[Q^2 F_\pi(Q^2)]^{res} \xrightarrow{Q^2 \rightarrow \infty} \frac{(16\pi f_\pi)^2}{\beta_0} B(2, 1) \int_0^{\infty} du e^{-ut} B(2, 1-u). \quad (5.6)$$

From Eqs. (5.6) and (3.8) we obtain

$$[Q^2 F_\pi(Q^2)]^{res} \xrightarrow{Q^2 \rightarrow \infty} 16\pi f_\pi^2 \alpha_s(Q^2), \quad (5.7)$$

which can be found in the context of the standard HSA by employing the pion asymptotic DA.

To perform the numerical analysis of the scaled and resummed pion FF $Q^2 F_\pi(Q^2)$ and extract constraints on the pion DA's from such consideration, we need to specify the experimental data that will be used in the fitting procedure. Unlike the $\pi^0 \gamma$ transition FF, where we have precise CLEO data for large momentum transfers, the situation with the $Q^2 F_\pi(Q^2)$ is somewhat controversial. Thus the corresponding data were obtained indirectly from the pion electroproduction experiments through a model-dependent extrapolation to the pion pole. Moreover, the points $Q^2 > 2 \text{ GeV}^2$ are imprecise suffering from the large errors and, in addition, there are big gaps between data points themselves. The data on the FF $Q^2 F_\pi(Q^2)$ reported recently by the F_π Collaboration do not change the whole picture, because the highest value of Q^2 at which the measurements were performed is $Q^2 = 1.6 \text{ GeV}^2$. Therefore, to improve the precision of the 1σ analysis under the circumstances, we include into our fitting procedure data points $Q^2 \geq 1.18 \text{ GeV}^2$ and slightly exceed in this way the range of validity of the RC method. But because our curves describe the data at such low values of Q^2 as well, we find our approach justified. Finally, let us note that the datum point $Q^2 = 9.77 \text{ GeV}^2$ is also included into our scheme and it strongly restricts the 1σ region.

The results of our numerical calculations are plotted in Figs. 5 and 2. The 1σ area for the pion scaled electromagnetic FF and the central curve with the Gegenbauer coefficients

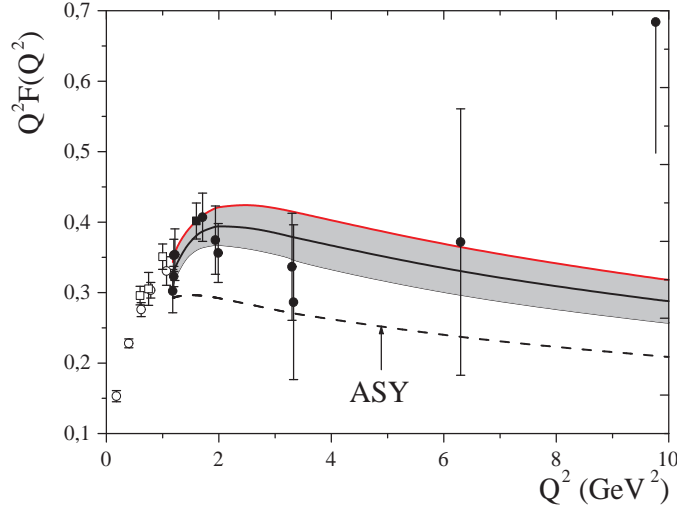


FIG. 5: The pion scaled and resummed electromagnetic FF $Q^2 F_\pi(Q^2)$ as a function of Q^2 . The shaded area is the 1σ region for the form factor. The data are taken from Refs. [28] (the circles) and [29] (the rectangles). In the 1σ analysis only the solid data points are used. For the central solid line the input parameters are $b_2^0 = 0.23$, $b_4^0 = -0.05$. For comparison the FF obtained by means of the asymptotic DA is also plotted.

$b_2^0 = 0.23$, $b_4^0 = -0.05$ are demonstrated in Fig. 5. The 1σ region for the parameters b_2^0 , b_4^0 of the pion DA's is shown in Fig. 2. They obey, for example, the following constraints

$$b_2^0 = 0.16, \quad b_4^0 \in [-0.045, -0.05],$$

$$b_2^0 = 0.2, \quad b_4^0 \in [-0.039, -0.058],$$

and

$$b_2^0 = 0.28, \quad b_4^0 \in [-0.047, -0.061].$$

The overlap of the 1σ regions in Fig. 2 determines the 1σ area in the plane $b_4^0 - b_2^0$, within which both the $\pi^0\gamma$ transition and the pion electromagnetic FF's are in agreement with the corresponding data at the level of a 1σ accuracy. As is seen, this area is rather restricted and the values of the parameters b_2^0 and b_4^0 are

$$b_2^0 = 0.235 \pm 0.035, \quad b_4^0 = -0.05 \mp 0.01. \quad (5.8)$$

The FF $Q^2 F_\pi(Q^2)$ is more sensitive to HT ambiguities than the $\pi^0\gamma$ transition FF. Actually, in Fig. 6 for $b_2^0 = 0.23$ and $b_4^0 = -0.05$ the scaled FF, corrected by the HT ambiguities, is plotted. These ambiguities for $\{N_q\} = 0.1$ and $\{N_q\} = -0.08$ reach $\pm(5.6 - 3.6)\%$ of the FF in the region $Q^2 \sim 1.2 - 1.6 \text{ GeV}^2$ and $\pm 1\%$ in the domain $9 - 10 \text{ GeV}^2$. It is worth noting that the estimation of the HT ambiguities are obtained within the " 1σ constraint" (see the previous section). In general, admissible values of the constants $\{N_q\}$ and of the input parameters b_2^0 , b_4^0 are strongly correlated.

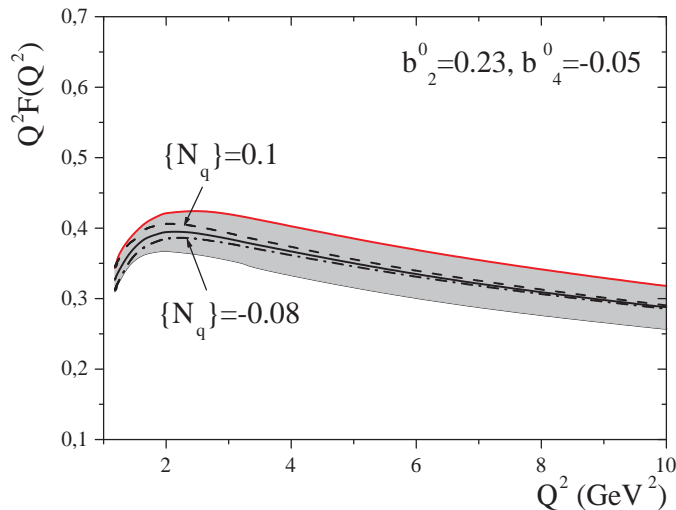


FIG. 6: The pion electromagnetic FF with HT ambiguities. The solid line is the original FF with $b_2^0 = 0.23$, $b_4^0 = -0.05$. The broken lines include the HT ambiguities with constants $\{N_q\} = 0.1$ (the dashed line) and $\{N_q\} = -0.08$, (the dot-dashed line) $q = 1, 2, \dots, 6$.

VI. CONCLUDING REMARKS

In this work we have calculated the power corrections to the $\pi^0\gamma$ transition FF, originating from the end-point regions $x \rightarrow 0, 1$ due to integration of the standard HSA factorization formula with the QCD running coupling over the longitudinal momentum fraction x , carrying by the pion's quark. To this end, we have employed the RC method combined with techniques of the IR renormalon calculus. We have used the symmetrized under replacement $\mu_R^2 \leftrightarrow \bar{\mu}_R^2$ version of the hard-scattering amplitude of the partonic subprocess $\gamma^* + \gamma \rightarrow q + \bar{q}$.

We have obtained the Borel resummed expression $[Q^2 F_{\pi\gamma}(Q^2)]^{res}$ for the transition FF. For this purpose in the inverse Borel transformation we have removed IR renormalon divergences by means of the principal value prescription. Each IR renormalon pole $u_0 = n$ in the Borel transform $B[Q^2 F_{\pi\gamma}](u)$ corresponds to power correction $\sim 1/Q^{2n}$ contained in the scaled and resummed FF. Since, in the considering process the Borel transform has an infinite number of IR renormalon poles, the expression (2.33), in general, contains power corrections $\sim 1/Q^{2n}$, $n = 1, 2, \dots, \infty$. In numerical computations we have truncated the corresponding series at $n_{\max} = 50$. As an important consistency check, we have proved that the result obtained within the SRC method in the asymptotic limit $Q^2 \rightarrow \infty$ reproduce the standard HSA prediction for the transition FF. This provides justification for the symmetrization procedure applied in the RC method.

We have compared our predictions with the CLEO data and obtained restrictions on the input parameters of the pion DA's with one and two nonasymptotic terms. Further constraints on the admissible set of DA's have been extracted from the data on the pion electromagnetic FF $F_\pi(Q^2)$. We have concluded that the pion DA's with the parameters Eq. (5.8) describe the experimental data on both the $Q^2 F_{\pi\gamma}(Q^2)$ and $Q^2 F_\pi(Q^2)$ FF's with the 1σ accuracy.

It is important that DA's extracted from the CLEO data are suitable for explanation of the pion electromagnetic FF, whereas in the context of the standard HSA for describing of these FF's one has to pose on the pion DA contradictory restrictions (or to model soft contributions to $F_\pi(Q^2)$ using mechanisms beyond the scope of the perturbative QCD). In fact, in the framework of the standard HSA the pion asymptotic DA considerably underestimates the data on the electromagnetic FF $Q^2 F_\pi(Q^2)$. In order to cover a gap between the data and theoretical curves one has to introduce model DA's with positive and large input parameters, the Chernyak-Zhitnitsky DA [17] being one of the prominent examples. At the same time, $\phi_{asy}(x)$ overestimates the CLEO data on $Q^2 F_{\pi\gamma}(Q^2)$ and, on the contrary, model DA's with negative input parameters are needed. The RC method solves this problem due to power corrections taken into account in both of these quantities. Really, the power corrections arising from the end-point integration regions at moderate momentum transfers significantly enhance the pion electromagnetic FF [12, 13]. They also enhance the absolute value of the NLO contribution to the FF $F_{\pi\gamma}(Q^2)$. Since the contribution of the NLO term to $F_{\pi\gamma}(Q^2)$ is negative, power corrections effectively reduce the leading order contribution to FF. It turns out that for some model DA's these effects lead to a satisfactory description for both of these FF's.

The investigation performed in this work has allowed us to describe the form factors $F_{\pi\gamma}(Q^2)$ (for $Q^2 \geq 1.64 \text{ GeV}^2$) and $F_\pi(Q^2)$ (for $Q^2 \geq 1.18 \text{ GeV}^2$) in the context of the same theoretical scheme and by means of the same DA's. We have achieved a quite satisfactory agreement with the available experimental data. Theoretical computations have been carried out using the leading order [for $F_\pi(Q^2)$] and the NLO [for $F_{\pi\gamma}(Q^2)$] expressions for the hard-scattering amplitudes of the partonic subprocesses. An accuracy of our theoretical predictions may be improved by including into analyses the NLO and NNLO terms, respectively. These problems form directions for improving the developed theoretical framework and require separate detailed investigations.

-
- [1] G. P. Lepage and S. J. Brodsky, Phys. Rev. D **22**, 2157 (1980).
 - [2] A. V. Efremov and A. V. Radyushkin, Theor. Math. Phys. **42**, 97 (1980) [Teor. Mat. Fiz. **42**, 147 (1980)]; Phys. Lett. B **94**, 245 (1980).
 - [3] A. Duncan and A. H. Mueller, Phys. Rev. D **21**, 1636 (1980).
 - [4] CLEO Collaboration, J. Gronberg et al., Phys. Rev. D **57**, 33 (1998) [hep-ex/9707031].
 - [5] S. S. Agaev and A. I. Mukhtarov, Int. J. Mod. Phys. A **16**, 3179 (2001).
 - [6] A. P. Bakulev, S. V. Mikhailov, and N. G. Stefanis, Phys. Lett. B **508**, 279 (2001) [hep-ph/0103119]; Phys. Rev. D **67**, 074012 (2003) [hep-ph/0212250].
 - [7] A. Schmedding and O. Yakovlev, Phys. Rev. D **62**, 116002 (2000) [hep-ph/9905392].
 - [8] P. Gosdzinsky and N. Kivel, Nucl. Phys. B **521**, 274 (1998) [hep-ph/9707367]; H. Diehl, P. Kroll, and C. Vogt, Eur. Phys. J. C **22**, 439 (2001) [hep-ph/0108220]; Y. V. Mamedova, Int. J. Mod. Phys. A **18**, 1023 (2003).
 - [9] S. S. Agaev, Phys. Rev. D **64**, 014007 (2001).
 - [10] S. J. Brodsky, G. P. Lepage, and P. B. Mackenzie, Phys. Rev. D **28**, 228 (1983).
 - [11] S. S. Agaev, Phys. Lett. B **360**, 117 (1995); **369**, 379(E) (1996).
 - [12] S. S. Agaev, Mod. Phys. Lett. A **10**, 2009 (1995); **11**, 957 (1996); **13**, 2637 (1998) [hep-ph/9805278].

- [13] S. S. Agaev, A. I. Mukhtarov, and Y. V. Mamedova, *Mod. Phys. Lett. A* **15**, 1419 (2000).
- [14] A. I. Karanikas and N. G. Stefanis, *Phys. Lett. B* **504**, 225 (2001) [hep-ph/0101031].
- [15] S. S. Agaev and N. G. Stefanis, *Eur. Phys. J. C* **32**, 507 (2004) [hep-ph/0212318].
- [16] F. del Aguila and M. K. Chase, *Nucl. Phys. B* **193**, 517 (1981); E. Braaten, *Phys. Rev. D* **28**, 524 (1983); E. P. Kadantseva, S. V. Mikhailov, and A. V. Radyushkin, *Sov. J. Nucl. Phys.* **44**, 326 (1986) [*Yad. Fiz.* **44**, 507 (1986)].
- [17] V. L. Chernyak and A. R. Zhitnitsky, *Phys. Rep.* **112**, 173 (1984).
- [18] G. R. Farrar, K. Huleihel, and H. Zhang, *Nucl. Phys. B* **349**, 655 (1991).
- [19] V. M. Braun and I. E. Filyanov, *Z. Phys. C* **44**, 157 (1989); *ibid*, *C* **48**, 239 (1990).
- [20] H. Contopanagos and G. Sterman, *Nucl. Phys. B* **419**, 77 (1994) [hep-ph/9310313].
- [21] G. 't Hooft, in *Whys of Subnuclear Physics*, Proceeding of the International School, Erice, 1977, edited by A. Zichichi (Plenum, New York 1978); A. I. Zakharov, *Nucl. Phys. B* **385**, 452 (1992).
- [22] B. R. Webber, *J. High Energy Phys.* **10**, 012 (1998) [hep-ph/9805484].
- [23] A. P. Prudnikov, Yu. A. Brychkov, and O. I. Marichev, *Integrals, and Series, Vol. 3; More Special Functions* (Gordon and Breach, New York, 1990).
- [24] S. S. Agaev, *Nucl. Phys. B (Proc. Suppl.)* **74**, 155 (1999) [hep-ph/9807444].
- [25] M. Beneke, *Phys. Rep.* **317**, 1 (1999) [hep-ph/9807443].
- [26] R. D. Field, R. Gupta, S. Otto, and L. Chang, *Nucl. Phys. B* **186**, 429 (1981); F.-M. Dittes and A. V. Radyushkin, *Sov. J. Nucl. Phys.* **34**, 293 (1981) [*Yad. Fiz.* **34**, 529 (1981)]; E. Braaten and S.-M Tse, *Phys. Rev. D* **35**, 2255 (1987).
- [27] H.-n. Li and G. Sterman, *Nucl. Phys. B* **381**, 129 (1992); S. W. Wang and L. S. Kisslinger, *Phys. Rev. D* **54**, 5890 (1996) [hep-ph/9608252]; G. Sterman and P. Stoler, *Annu. Rev. Nucl. Part. Sci.* **47**, 193 (1997) [hep-ph/9708370]; N. G. Stefanis, W. Schroers, and H. C. Kim, *Eur. Phys. J. C* **18**, 137 (2000) [hep-ph/0005218].
- [28] C. J. Bebek et al., *Phys. Rev. D* **17**, 1693 (1978).
- [29] J. Volmer et al., *Phys. Rev. Lett.* **86**, 1713 (2001) [nucl-ex/0010009].